Analysis of the ST-T complex of the electrocardiogram using the Karhunen–Loève transform: adaptive monitoring and alternans detection

P. Laguna[1] G. B. Moody[2] J. García[1] A. L. Goldberger[3] R. G. Mark[2]

[1]Grupo de Tecnologías de las Comunicaciones, Departamento de Ingeniería Electrónica y Comunicaciones, Centro Politécnico Superior, Universidad de Zaragoza, C/Maria de Luna 3, 50015 Zaragoza, Spain

[2]Division of Health Sciences & Technology, Harvard–Massachusetts Institute of Technology, Cambridge, MA, USA

[3]Cardiovascular Division, Beth Israel Hospital–Harvard Medical School, Boston, MA, USA

Abstract—*The Karhunen–Loève transform (KLT) is applied to study the ventricular repolarisation period as reflected in the ST-T complex of the surface ECG. The KLT coefficients provide a sensitive means of quantitating ST-T shapes. A training set of ST-T complexes is used to derive a set of KLT basis vectors that permits representation of 90% of the signal energy using four KLT coefficients. As a truncated KLT expansion tends to favor representation of the signal over any additive noise, a time series of KLT coefficients obtained from successive ST-T complexes is better suited for representation of both medium-term variations (such as ischemic changes) and short-term variations (such as ST-T alternans) than discrete parameters such as the ST level or other local indices. For analysis of ischemic changes, an adaptive filter is described that can be used to estimate the KLT coefficient, yielding an increase in the signal-to-noise ratio of 10 dB ($u = 0.1$), with a convergence time of about three beats. A beat spectrum of the unfiltered KLT coefficient series is used for detection of ST-T alterans. These methods are illustrated with examples from the European ST-T Database. About 20% of records revealed quasi-periodic salvos of ischemic ST-T change episodes and another 20% exhibit repetitive, but not clearly periodic patterns of ST-T change episodes. About 5% of ischemic episodes were associated with ST-T alternans.*

Keywords—*ST level, ST-T complex, Ischaemia, KL transform, Alternans, Monitoring*

Med. Biol. Eng. Comput., 1999, **37**, 175–189

1 Introduction

ELECTROCARDIOGRAPHIC (ECG) information is derived from analysis of both the depolarisation (QRS complex) and repolarisation (ST-T waveform) phases of the cardiac electrical cycle. Considerable interest has been directed at ventricular repolarisation (VR) in recent years because subtle ST-T changes can be a marker of electrical instability that may result in increased susceptibility to ventricular fibrillation (VF) and sudden cardiac death (SCD) (ROSENBAUM *et al.*, 1994 Repolarisation can be perturbed by multiple factors, including ischaemia, structural heart disease, metabolic factors (e.g. electrolyte abnormalities, drugs) and neurohumoral factors.

At present, there are no generally accepted non-invasive indices of the risk of SCD, although such indices would have very substantial implications for both public health policy and medical practice, and many studies have sought to develop such indices. Among the most promising candidates are measurements of heart rate variability (HRV) (KLIEGER *et al.*, 1984; MYERS *et al.*, 1986), ventricular late potentials (BERBARI and LAZZARA, 1988; BREITHARDT *et al.*, 1991), repolarisation duration (QT) interval (PUDDU and BOURASSA, 1986), QT variability (MERRI *et al.*, 1993; SPERANZA *et al.*, 1993), assessment of heterogeneity of repolarisation (QT dispersion) in different leads, and repolarisation alternans (CLANCY *et al.*, 1991; ROSENBAUM *et al.*, 1994) (a possible precursor of ventricular fibrillation). Except for the first two, all of these indices are derived from the ST-T complex of the ECG, which has long been known as a highly sensitive (though arguably less predictive) marker of myocardial ischaemia (GALLINO *et al.*, 1984; AKSELROD *et al.*, 1987).

Most of these indices to describe VR are derived from discrete features of the ST-T complex, a practice that reflects the difficulty of deriving integrated measurements using visual analysis. However, the ST-T waveform represents a complex spatial and temporal summation of electrical potentials from innumerable ventricular cells. Therefore, if physiologically and

Correspondence should be addressed to P. Laguna
email: laguna@posta.unizar.es

First received 22 June 1998 and in final form 27 October 1998

clinically relevant information is contained within the ST-T complex, this information may not necessarily be concentrated within any individual differential feature or subinterval such as ST levels and QT intervals, but may be represented by the entire ST-T waveform.

The proliferation of additional 'heuristic' measurements that describe the ST-T complex shape clearly demonstrates the need to consider more than the traditional measurements to characterise subtle changes in VR. Furthermore, noise and other sources of measurement error (such as errors in fiducial or baseline estimation) have far more deleterious effects on measurements of isolated features and simple differential measurements than on integrated measurements. These considerations, together with the increasing evidence for the importance of repolarisation alterations as a marker of electrical instability and SCD, led us to consider the objective of developing an analytic technique based on the entire ST-T complex.

We chose to use the Karhunen–Loève transform (KLT), which has the power to characterise the shape of the entire ST-T complex, and which is minimally affected by noise. We propose that a feature set of KLT coefficients would provide a superior method for characterising each beat, and that the KLT feature set would provide a much more sensitive and robust quantisation of ST-T shape than the discrete measures commonly used in clinical practice, such as ST or QT measures.

In a previous study (JAGER *et al.*, 1992), the KLT was successfully applied to analyse the ST segment of the ECG, with the specific aim of obtaining noise-tolerant methods for ischaemia detection. In this study, we have applied the KLT to the entire ST-T complex, to include as much information about VR as possible, with the broader aim of noise-tolerant characterisation of both beat-to-beat and longer-term variations in VR.

In the following Sections, we describe our technique for ST-T complex representation, including construction of KLT basis functions and derivation of KL_n coefficient time series $kl_n(i)$. We also present an adaptive filter (LAGUNA *et al.*, 1996*a*; THAKOR *et al.*, 1993), suitable for estimating the $kl_n(i)$ time series, that reduces the noise of the $kl_n(i)$ estimation while preserving the deterministic coefficient information. We apply these techniques to ECG records from the European ST-T database, and we show how the first and second $kl_n(i)$ ($n = 0, 1$) series can be used to monitor ST segment changes in these records. We illustrate this point with examples of periodic behaviour of the ischaemic process within these records. We also analyse the power spectral density (PSD) of the $kl_n(i)$ series. This analysis is made using PSD estimation of the $kl_n(i)$ coefficients expressed with temporal reference to the beat order (DEBOER *et al.*, 1984) (as previously used for HRV analysis) rather than the beat occurrence time t_i. This analysis also points out the possibility of detecting ventricular alternans using the peaks of the spectrum at 0.5 beats^{-1} 'beatquency'. We show examples (from the European ST-T database) of the appearance of alternans in association with ischaemic ST and T-wave changes that were successfully detected by this method.

2 The Karhunen–Loève transform applied to ST-T complex

The KLT (HADDAD and PARSONS, 1991) is a signal-dependent linear transform that is optimum in the following sense: for a given signal (an ST-T complex) lasting N samples and any given number of parameters $n \leqslant N$, if the signal is reconstructed from the first n terms of the series expansion of a linear transformation, the lowest expected mean-squared error will be obtained if the transform is chosen to be the KLT.

The KLT thus has two major advantages over other linear transforms: it concentrates the signal information in the minimum number of parameters and it defines the domain where the signal and noise are most separated. These properties are obtained at the expense of generality, however: it is by estimation of the 'most likely' variations in waveform shape that the KLT acquires its property of noise rejection.

A KLT for a given type of signal must be derived from the statistics of examples of that signal; it is unlikely to be useful (with the same optimum properties) for analysis of other types of signal. Thus, a significant constraint of the KLT is that it is necessary to collect a representative 'training' set of the signals to be analysed, to derive the KLT basis functions (eigenfunctions). The performance of the KLT, in terms of capacity to concentrate information in a small coefficient set, depends on how well the training set has been constructed. Once each ST-T complex is characterised by n kl coefficients, we construct n kl series ($kl_n(i)$) as the series formed by the kl coefficients of the i*th* beat.

In this Section we describe our technique for analysing the ST-T complex using the KLT. First, we discuss the derivation of the training set, including the preprocessing performed on the ECG to attenuate noise and to exclude beats likely to be significantly corrupted by noise. We then present an adaptive filter for estimating the $kl_n(i)$ series of an ECG record.

In this work, we represent each ST-T complex first by a pattern vector, $\boldsymbol{x}$, whose components are the time-ordered samples of the ST-T complex (after baseline correction and normalisation, described below). The KLT is a rotational transformation of a pattern vector into a feature vector, whose components are the KLT coefficients. As shown below, the first few components of the feature vector represent almost all of the signal energy, and the remaining components need not even be computed.

The derivation of the KLT basis functions begins with estimation of the covariance matrix $\boldsymbol{C}$ of the pattern vectors of the training set (HADDAD and PARSONS, 1991).

$$\boldsymbol{C} = E\{(\boldsymbol{x} - \boldsymbol{m})(\boldsymbol{x} - \boldsymbol{m})^T\} \quad (1)$$

where $\boldsymbol{m}$ is the mean pattern vector over the entire training set. The covariance matrix reflects the distribution of the pattern vectors in the pattern space. The orthogonal eigenvectors of $\boldsymbol{C}$ are the basis functions of the KLT, and the eigenvalues λ_k, represent the average dispersion of the projection of a pattern vector onto the corresponding basis function.

After sorting the eigenvectors in order by their respective eigenvalues, such that $\lambda_k \geqslant \lambda_{k+1}$, for $k = 0, 1, \ldots, N-1$, the corresponding basis functions are arranged in order of representational strength. The basis function corresponding to the largest eigenvalue is that function best able to represent an arbitrary pattern vector from the training set; the next function is the (orthogonal) function best able to represent the residual error obtained from fitting the first function etc.

The value of N is equal to the number of components in the pattern vector and depends on the length of the waveform and on the sampling frequency; in this case, the length is 600 ms, and the sampling frequency is 250 Hz, so that $N = 150$.

In this study, the mean pattern vector $\boldsymbol{m}$ can be forced to be zero, if we assume that each ST-T complex in the training set can represent both itself and its inverted counterpart. This represents the possibility that any ST-T complex may appear inverted simply as an artefact of the choice of the lead polarity when the ECG is recorded. Thus, the covariance matrix can be expressed simply as

$$\boldsymbol{C} = E\{(\boldsymbol{x})(\boldsymbol{x})^T\} \quad (2)$$

and the eigenvalues, rather than representing the average dispersion of the ST-T projection onto the associated basis function, instead represent the average energy of this projection.

2.1 *Derivation of training set and KL_n basis functions*

To obtain a representative training set of normal and abnormal ST-T waveforms, we selected a wide variety of ECG records, totalling 105 in all (LAGUNA *et al.*, 1997): 15 from the MIT-BIH Arrhythmia Database (MOODY and MARK, 1990*a*); six from the MIT-BIH ST Change Database; 13 from the MIT-BIH Supra-ventricular Arrhythmia Database; ten recordings of healthy subjects from BIH; 33 from the European ST-T Database (TADDEI *et al.*, 1992), four from the MIT-BIH Long-term Database; and 24 from SCD recordings collected at BIH, which included a wide spectrum of T-wave shapes, ST elevation, ST depressions etc.

From each of these 105 recordings, a 15 min excerpt was selected. As the noise discrimination power of the KLT depends on the distribution of the pattern vectors as reflected in the covariance matrix, we tried to avoid including segments that were obviously corrupted by baseline wander or other noise.

From these 105 15 min records, we selected the training set of ST-T complexes according to the following procedure. First, QRS complexes were detected and labelled using ARISTOTLE software (MOODY and MARK, 1982). Each detected QRS complex was marked at a fiducial point corresponding to the centre of gravity of the significant peaks of the convolution of the QRS complex with the QRS detection function, a matched filter characterised by a W-shaped impulse response. This method of fiducial point placement was chosen for its stability with respect to minor morphology changes, as in respiration-related axis shift, as well as for its tolerance of impulse noise. The QRS fiducial points generally coincide with the R-wave peaks of monophasic QRS complexes and lie between the major positive and negative deflections of biphasic QRS complexes.

We defined the ST-T complex as the portion of the signal within a window beginning 85 ms following a QRS mark q_i, and ending 240 ms prior to the next QRS mark q_{i+1}. If the RR interval rr_i (defined as the interval between the QRS marks) is less than 720 ms, the end of the window is located at $q_i + \frac{2}{3}rr_i$ (i.e. two-thirds of the way from the initial QRS mark to the following one). This strategy permits inclusion of the whole ST-T complex, independently of the QT duration. (The ST-T window is restricted to 600 ms.)

In those cases where T-waves end later than 240 ms prior to the next QRS mark, it is very likely that the T-waves are distorted by the next P-wave. It is better to exclude those beats rather than have them corrupt the training set. These values have been selected according to the clinical values of intervals and from our experimental work when deriving the KLT of the ST-T complex. When we refer to ST-T as defined here we include the U wave, in the cases where it exists (this will be observed later when discussing Fig. 2).

To avoid the effects of ectopic and other abnormal beats on the ST-T complex, we accepted only ST-T complexes associated with QRS complexes labelled as normal by ARISTOTLE (MOODY and MARK, 1990*b*), and we further required that both the previous and following QRS complexes also be labelled as normal.

For each beat, we estimated the iso-electric level in the PR interval as the signal averaged during the 20 ms interval beginning 80 ms prior to the QRS mark. This iso-electric value, measured in the different beats, was used as input to the cubic spline interpolation of the ECG signal in the baseline cancellation (MEYER and KEISER, 1977). Beats for which the estimated iso-electric level differed by more than 0.2 mV from that of the previous or following beat were excluded from the training set.

The presence of delta waves associated with pre-excitation (Wolff–Parkinson–White syndrome) in four records required us to use intervals beginning 100 ms (records sel50, sel308, and sel17152) or 120 ms (record sel230) prior to the QRS mark for the iso-electric level estimation in these cases. We then manually rejected a small number of ST-T complexes that we judged subjectively to be particularly noisy. The remaining $97\,663 \times 2$ leads ST-T complexes formed the training set.

We generated the set of pattern vectors for the training set in six different ways, to test the effects of ST-T dependence on heart rate (HR) and of noise on the KLT representation. We used both uniformly sampled ST-T complexes and complexes corrected with Bazett's formula (BAZETT, 1920) and then resampled. We corrected for baseline variation using cubic splines and using a high-pass filter. (As the KLT basis functions will be influenced by incorrectly determined iso-electric levels, we selected recordings with minimum baseline variation. Even in such recordings, however, it is still necessary to account for baseline variation caused by respiration.) Finally, given the low-frequency content of the ST-T complex (THAKOR *et al.*, 1984), we also studied the effects of bandpass filtering the ECG signal as a means of improving the signal-to-noise ratio. These considerations led us to develop six sets of pattern vectors from the training set:

Set 1: Cubic splines were used for baseline removal (MEYER and KEISER, 1977). The knots were taken to be the centres of the iso-electric intervals, as defined above.

Set 2: As in set 1, but we corrected for the effects of heart rate on the ST-T complex using Bazett's formula. This is performed by resampling within the ST-T window at a sampling frequency equal to the original (250 Hz) divided by $\sqrt{rr_i}$, where rr_i is the previous RR interval and is expressed in seconds. The result is a corrected ST-T complex $STT_c(t') = STT(t/\sqrt{rr_i})$.

Set 3: A second-order highpass filter (LYNN, 1977) was used, with a cutoff frequency of 1 Hz for baseline removal.

Set 4: As in set 3, but with HR correction as in set 2.

Set 5: Bandpass filtering was used: a highpass filter, as in set 3, together with a second-order lowpass filter (−3 dB at 28 Hz) for attenuation of high-frequency noise.

Set 6: As in set 5, but with HR correction as in set 2.

In each case, the pattern vectors were normalised by magnitude (i.e. scaled such that the signal energy was constant); in this way, each pattern vector is accorded equal importance when the KLT basis functions are derived.

As the durations of the ST-T complexes vary (the final part of the ST-T complex is not always available, owing to the appearance of the next P-wave and QRS complex), the estimation of certain elements of the covariance matrix is problematic. Although it would be possible to extend the pattern vectors (by adding zero elements) so that all are of equal length, this procedure would tend to reduce the significance of non-zero elements in these positions when they are available, thereby lending an artefactual bias in favour of the initial elements. We prefer to address this issue by estimating each element of the covariance matrix using only those ST-T complexes for which the corresponding elements are available. This procedure avoids introducing artefacts of the window definition into the covariance matrix estimate; its consequence is that the final portions of the derived basis functions are derived from a smaller sample than the initial portions.

In Fig. 1 we plot the cumulative eigenvalue energy (CEE)

$$CEE(n) = 100 \frac{\sum_{k=0}^{n} \lambda_k}{\sum_{k=0}^{N-1} \lambda_k} \quad (3)$$

as a function of the KL_n order n, for the KLT basis functions derived using pattern vector set 1 (with cubic spline baseline correction), and for the KLT basis functions derived using set 2 (with correction for heart rate). Note how the CEE for set 2 is higher than the CEE for set 1 for low values of n, reflecting the reduction in waveform variability once the effects of heart rate are (at least in part) accounted for. This results in representing approximately 5% more energy by the first two HR corrected basis functions than by their uncorrected counterparts (Fig. 1).

In the training set, the average HR is quite low, as a result of our requirement of minimum baseline wander (generally accompanying low levels of physical activity and consequent low HR). This works to the disadvantage of the set 1 basis functions, as there is relatively little representation of ST-T complexes corresponding to high HR, with energy concentrated in the initial part of the window. The HR-corrected pattern vectors corresponding to ST-T complexes in high HR, however, closely resemble those in set 2, and are thus better represented by the low-order KLT coefficients of set 2 than those of set 1 (for an example, see Section 2.2).

Although correction for HR produces an improvement in the quality of the KLT, we do not observe any improvement using high-pass or bandpass filtering (pattern vector sets 3–6). This result agrees with the supposition that the KLT is the most effective linear method for separating the signal from the noise, and that any other linear filter cannot produce further improvements. Cubic spline correction of baseline variation produced slightly better results than high-pass filtering.

The first 14 KLT basis functions are displayed in Fig. 2 for the uncorrected set 1 (solid lines) and for the corrected set 2 (broken lines). It is apparent that the energy in the corrected set is concentrated at a later time than that in the uncorrected set. As most heart rates exceed 60 beats min^{-1}, the correction applied to most ST-T complexes tends to stretch them (i.e. to move the concentration of energy towards the end of the window).

The first basis function and, to a lesser extent, the second one represent the dominant low-frequency components of the ST-T complex concentrated in the first 400 ms after the QRS. The next few basis functions contain more high-frequency energy and contain energy more evenly distributed across the entire complex. These functions represent components present in abnormally prolonged ST-T complexes and in U-waves, where present within the window. The remaining higher-order basis vectors shown in Fig. 2 contain almost exclusively high-frequency content related to noise in the training set.

By inspection of the basis vectors, we can predict that the first two KLT coefficients $kl_0(i)$ and $kl_1(i)$ should be a good tool for detecting ischaemic ST-T changes, as they contain virtually all of the low-frequency energy; we discuss this point further in Section 3.2. Also, looking to the basis 0, it is apparent that it will mostly represent ST segment elevation waveforms (has a positive value at the ST segment) that will result in positive $kl_0(i)$ values; in contrast, basis 1 (has a negative value at the ST segment) will represent ST segment depression waveforms resulting in positive $kl_1(i)$ values.

2.2 *KLT representation of the ST-T complex*

To illustrate the ability of the KLT to represent an arbitrary ST-T complex, we will analyse in this section the reconstruction of several real ST-T complexes.

In Fig. 3, we present the reconstruction of three ST-T complexes with three, five and eight KLT coefficients, using both set 1 (uncorrected) and set 2 (HR-corrected) KLT basis functions. The first complex (Figs. 3*a* and *b*) includes a prominent U-wave. As high amplitude of U-waves was unusual in the training set, a faithful reconstruction requires more than the first few KLT coefficients. The RR interval in this case is 1228 ms, implying only a small HR correction; we see, however (Fig. 3*b*), how this small shift to the left results in a markedly better reconstruction with the low-order coefficients. At the right, the cumulative signal energy ($CE(n) = 100 \sum_{j=0}^{n} kl_j^2 / \sum_{k=0}^{N-1} STT^2(k)$) is shown for each reconstruction.

Figs. 3*c* and *d* show an ST-T complex during high HR (RR = 440 ms). The signal energy is concentrated in the earliest part of the ST-T, and is poorly represented by the uncorrected KLT coefficients (Fig. 3*c*). The HR correction in this case shifts the ST-T complex to the right, producing a much better representation with the first three coefficients (Fig. 3*d*). This example shows the value of HR correction in cases where the HR is quite far from typical values.

Finally, Figs. 3*e* and *f* present the reconstruction of a biphasic ST-T complex with RR = 812 ms. Given that this shape is not dominant in the training set, more coefficients are required, for an accurate reconstruction, than in typical cases. The HR correction in this case is small, but a small improvement in the low-order reconstruction is still obtained. There always remains the question of how many coefficients are needed for an accurate reconstruction. For very rare wave-shapes (that can always occur), a much larger number of KLT coefficients may be required, but, in our studies, we did not find clinically significant wave-shapes that were not well reconstructed overall with the first three to four coefficients.

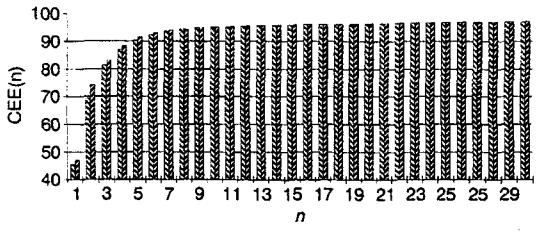

Fig. 1 *Cumulative eigenvalue energy* $CEE(n) = 100 \sum_{k=0}^{n} \lambda_k / \sum_{k=0}^{N-1} \lambda_k$ *as function of the sorted eigenvalue order n.* $N = 150$ *is total number of eigenvalues* λ_k. *(▨) Results obtained using pattern vector set 1 (baselines corrected using cubic splines); (▨) Results obtained using set 2 (with correction for heart rate)*

3 Monitoring the $kl_n(i)$ series

In the preceeding Section, we described how to derive a KLT representation of a single ST-T complex. In clinical practice, the dynamic behaviour over time of ST-T morphology is even more important than the characteristics of an isolated complex. ST-T dynamics can be characterised by the study of KLT coefficient time series $kl_n(i)$, using many of the techniques used in studies of HRV. We can assign to each beat mark (QRS fiducial point) the KLT coefficients of its ST-T complex. In this way we will have as many (scalar) time series as there are KLT coefficients needed to represent the ST-T complex.

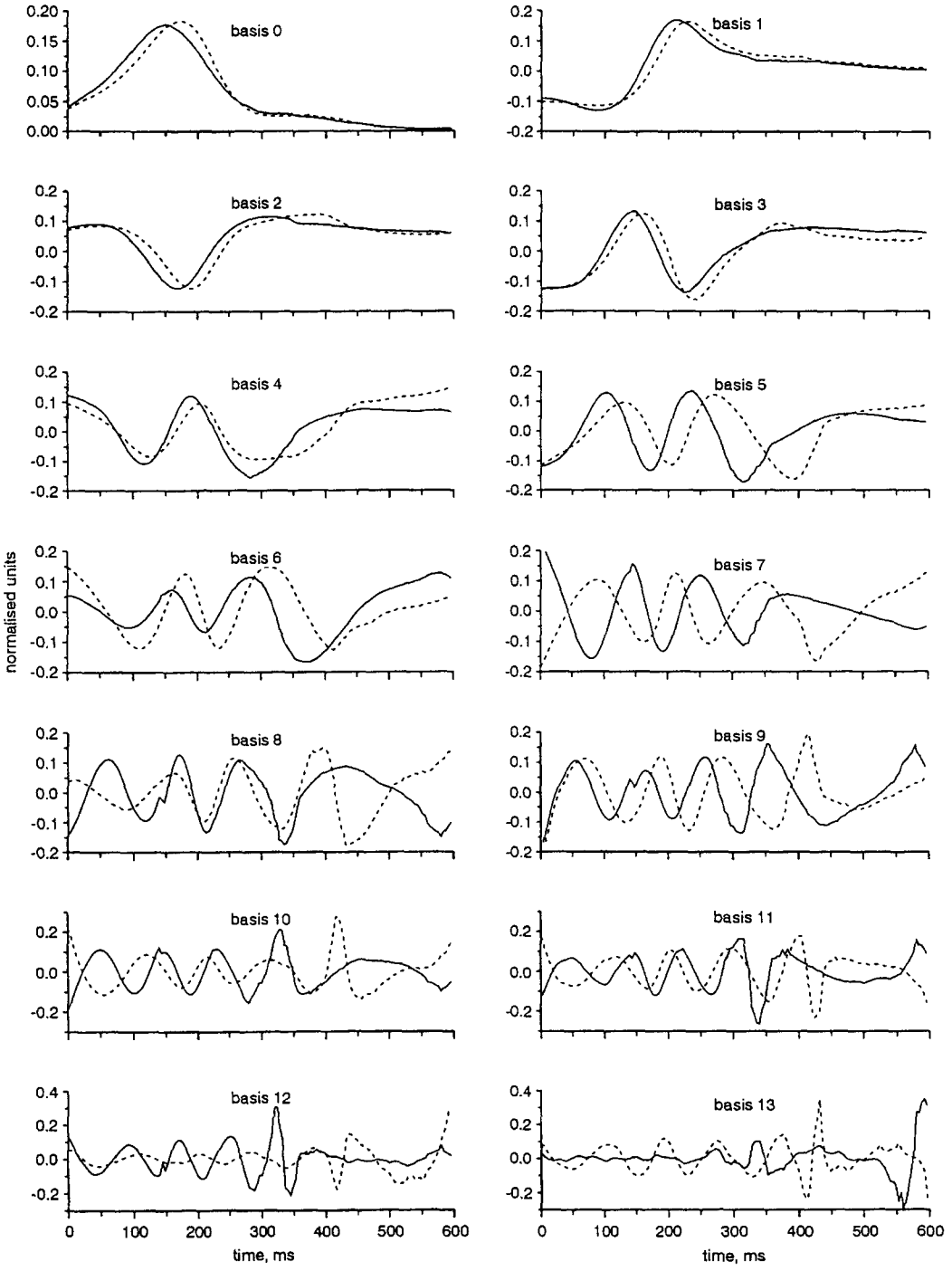

Fig. 2 *KLT basis functions. (——) functions derived from set 1 (without HR correction), (- - - -) functions derived from set 2 (with HR correction). Units of vertical axis are normalised (not mV), as the basis needs to be orthonormal, and have been multiplied by a normalising factor*

The direct way to monitor $kl_n(i)$ is to obtain it from the inner product of the KLT basis with the pattern vectors of the ST-T complexes to be analysed. These pattern vectors are obtained in the same manner as those in the training set (using cubic spline baseline removal, and HR correction if we are using the set 2 KLT). In this case, however, we do not normalise the energy of the ST-T complex pattern vectors, as we are interested in monitoring variations in energy as well as in morphology. We are not as restrictive as in the training set about rejecting beats, as now the obtained kl_n will influence only the beat that is represented and will not affect the others, as could happen if considered at the training set. The inner product is performed over the interval in which the ST-T complex is defined (not necessarily the entire window over which the basis function extends); this policy is equivalent to appending additional zero components to the pattern vector, as needed, to match its length to that of the basis function (see Section 2.1).

Direct estimation in this way, however, results in a noisy $kl_n(i)$ time series. Noise is introduced into the $kl_n(i)$ time series from a variety of sources, including noise in the ST-T complexes not removed by the KLT, residual error in the KLT domain representation of the ST-T complexes, mis-estimation of the iso-electric level (because of noise in the PR interval, or QRS fiducial mis-estimation), residual baseline variations and ectopic beats not rejected. Noise in the $kl_n(i)$ time series can be reduced using an adaptive filter that removes

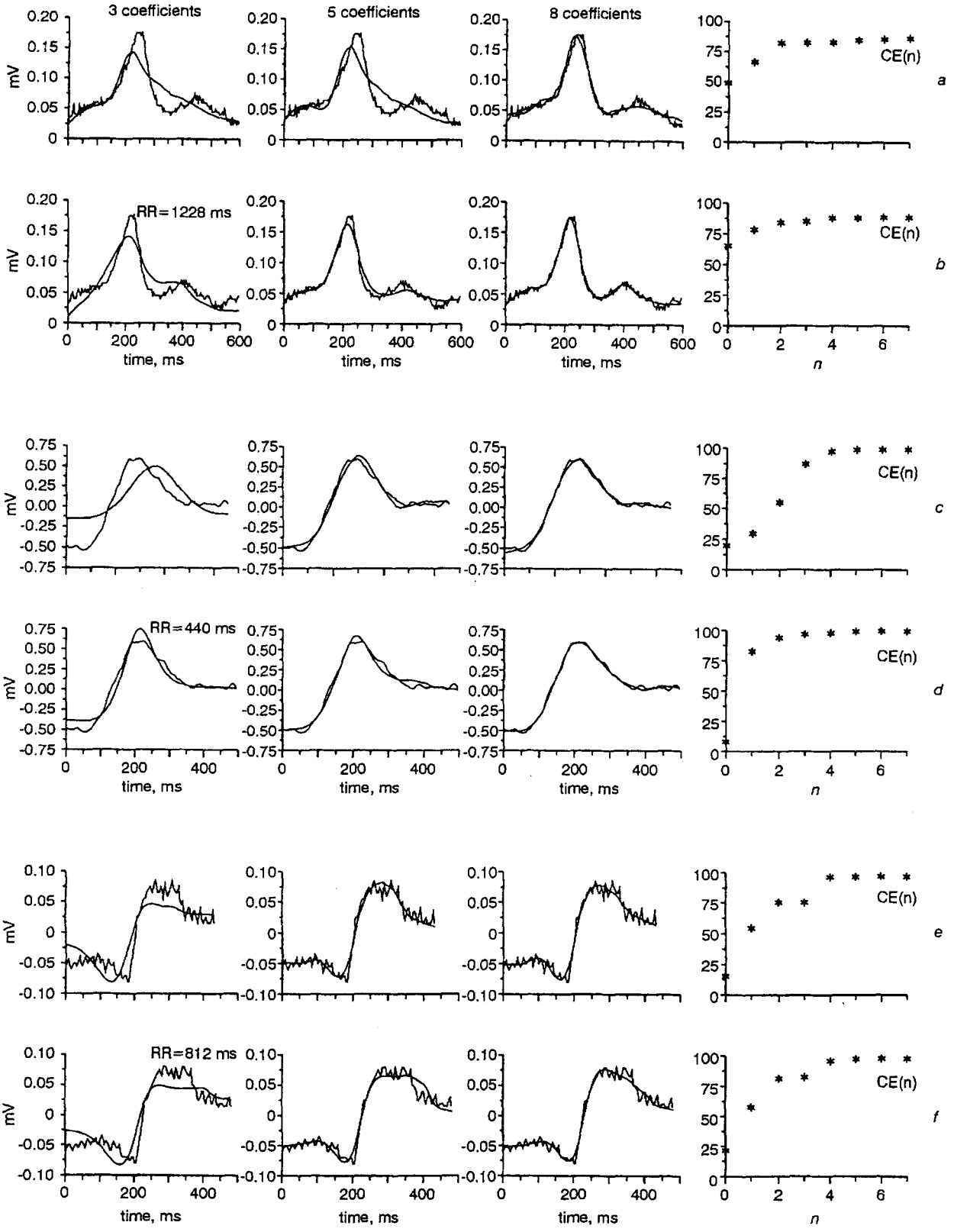

Fig. 3 *Reconstruction of three ST-T complexes with KLT. (a) ST-T complex with U-wave and its reconstruction based on three, five and eight KLT coefficients, together with cumulative energy (CE(n)) as function of $kl_n(i)$ order (n), plotted on right. (a) Uncorrected (set 1) KLT; (b) same ST-T complex, reconstructed using HR-corrected (set 2) KLT. (c), (d) and (e), (f), show similar reconstructions for two other ST-T complexes; see text for descriptions*

noise uncorrelated with the ST-T complex. This technique is useful for monitoring medium- to long-term variations in the ST-T complex, such as for detecting ischaemic ST-T changes; on the other hand, when we are interested in beat to-beat variations (alternans), direct $kl_n(i)$ estimation is necessary.

3.1 *Adaptive $kl_n(i)$ estimate*

Adaptive estimation of quasi-periodic signals such as the ST-T complex permits reduction of noise uncorrelated with the signal, with attendant improvements in the ability to track

subtle dynamic variations in these signals. This technique has been applied to analysis of ECG signals (LAGUNA *et al.*, 1992; 1996*a*) and evoked potentials (THAKOR *et al.*, 1993). It makes use of the recurring features of the signal and is based on the adaptive linear combiner (WIDROW and STEARNS, 1985).

In effect, the adaptive filter input signal (the primary input d_k) consists of concatenated ST-T complexes only, with all intervening data removed. Short complexes are lengthened by appending zeros as necessary, so that a new complex begins every N samples. The adaptive system dynamically estimates the amount of each reference input present in the input signal. In LAGUNA *et al.* (1996*a*), the reference inputs used for the estimation of the deterministic signal were the orthonormal Hermite functions; in LAGUNA *et al.* (1992), the reference inputs were unit impulses and, in THAKOR *et al.*, (1993) they were sine, cosine and Walsh functions. In the present study, the reference inputs are the KLT basis functions to be used to represent the ST-T complexes.

Fig. 4 shows this process in schematic form. We define the beginning of each ST-T complex (85 ms following the QRS fiducial mark in each case) as the time of the stimulus. The N samples that follow the stimulus are assumed to be the sum of the signal of interest (a deterministic signal component $s_k = STT_k$, correlated with the stimulus) and an uncorrelated noise component n_k. If the deterministic component is strictly periodic with a period of N samples, then it satisfies $s_k = s_{k+N}$ for all k.

The reference inputs KL_{jk} $(j = 0, \ldots, n-1)$ $(n \leqslant N)$ are formed by concatenating copies of the jth KLT basis function to be used to represent the ST-T complexes; thus $KL_{jk} = KL_{jk+N}$.

In the KLT vectorial space, d_k can be expressed as the sum of all the KLT components and the uncorrelated noise:

$$d_k = \sum_{j=0}^{N-1} kl_j KL_{jk} + n_k \tag{4}$$

The output of the adaptive filter y_k, is the signal that we want to be an estimate of s_k, and e_k is the error signal $e_k = s_k + n_k - y_k$ with

$$y_k = \sum_{j=0}^{n-1} w_{jk} KL_{jk} \tag{5}$$

If $\boldsymbol{KL}_k$ denotes the vector of reference inputs, and $\boldsymbol{W}_k$ denotes the weight vector:

$$\begin{aligned} \boldsymbol{KL}_k &= [KL_{0\,k}, KL_{1\,k}, \ldots, KL_{n-1\,k}]^T \\ \boldsymbol{W}_k &= [w_{0\,k}, w_{1\,k}, \ldots, w_{n-1\,k}]^T \end{aligned} \tag{6}$$

then

$$y_k = \boldsymbol{KL}_k^T \boldsymbol{W}_k = \boldsymbol{W}_k^T \boldsymbol{KL}_k \tag{7}$$

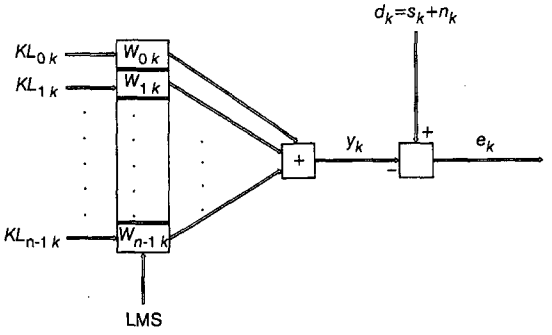

Fig. 4 *Adaptive estimation system for $kl_n(i)$*

Minimising the mean squared error $\xi = E[e_k^2]$ using any adaptive algorithm (WIDROW and STEARNS, 1985), the weight vector converges to the optimum solution $\boldsymbol{W}^* = \boldsymbol{R}^{-1}\boldsymbol{P}$ (WIDROW and STEARNS, 1985), where

$$\boldsymbol{R} = E[\boldsymbol{KL}_k \boldsymbol{KL}_k^T] \qquad \boldsymbol{P} = E[d_k \boldsymbol{KL}_k] \tag{8}$$

In this case, given the orthonormality conditions of the base elements of KLT vectorial space and (by definition) the lack of correlation between the noise n_k and the KLT basis $KL_{n\,k}$, $\boldsymbol{R}$ and $\boldsymbol{P}$ reduce to

$$\boldsymbol{R} = \frac{1}{N}\boldsymbol{I} \qquad \boldsymbol{P} = \frac{1}{N}[kl_0, kl_1, \ldots, kl_{n-1}]^T \tag{9}$$

and the optimum weight vector $\boldsymbol{W}^*$, which minimises the mean squared error $\xi = E[e_k^2]$, is given by

$$\boldsymbol{W}^* = [kl_0, kl_1, \ldots, kl_{n-1}]^T. \tag{10}$$

This result means that each weight w_i is an estimate of the ith KLT coefficient for s_k. Thus the weight vector is a characterisation of the deterministic signal component, and the output signal y_k, in the optimum case, takes the value

$$y_k = \sum_{j=0}^{n-1} w_i^* KL_{jk} = \sum_{j=0}^{n-1} kl_j KL_{jk} \tag{11}$$

i.e. the projection of s_k onto the subspace spanned by KL_{jk} $(i = 0, \ldots, n-1)$ with $n \leqslant N$. Thus y_k is the nth-order KLT representation of s_k, and $y_k = s_k$ if $n = N$ (i.e. if all of the KLT components are included).

The minimum mean squared error ξ_{min}, will be

$$\xi_{min} = E[d_k^2] - \boldsymbol{P}^T \boldsymbol{W}^* \tag{12}$$

Given that the weight vector oscillates around this optimum value, y_k is an unbiased estimate of s_k. The remaining noise due to the misadjustment M depends upon the adaptive algorithm used to adjust the weight vector (WIDROW and STEARNS, 1985). The elements of the weight vector, evaluated at the end of each ST-T complex, are the adaptive estimates of the KLT coefficients of that complex. The quality of the y_k estimation is thus directly related to the quality of the KLT estimation.

In this study, we have used the least mean squares (LMS) algorithm (WIDROW and STEARNS, 1985)

$$\boldsymbol{W}_{k+1} = \boldsymbol{W}_k + 2\mu e_k \boldsymbol{KL}_k \tag{13}$$

The condition that assures the convergence of the algorithm is (FEUER and WEINSTEIN, 1985)

$$0 < \mu < \frac{1}{3\ tr[\boldsymbol{R}]} = \frac{N}{3n} \tag{14}$$

The time constant τ_{mse} for the convergence of the MSE is

$$\tau_{mse} = \frac{1}{4\mu\lambda} = \frac{N}{4\mu} \tag{15}$$

where $\lambda = 1/N$ is the eigenvalue of the matrix $\boldsymbol{R}$ (all the eigenvalues are identical). τ_{mse} is expressed in sampling intervals. The gain constant μ thus controls the stability and the speed of convergence. The estimate of the weight vector can be obtained within a single beat, given an appropriate choice of μ that satisfies ($\tau_{mse} < N$) if necessary. Thus adaptive filtering can be used, in principle, even for tracking beat-by-beat ST-T variations.

To measure the excess of mean squared error, we calculate the misadjustment (WIDROW and STEARNS, 1985)

$$M = \frac{ExcessMSE}{\xi_{min}} \tag{16}$$

which, for the LMS algorithm, can be approximated by (WIDROW and STEARNS, 1985)

$$\boldsymbol{M} \simeq \mu\, tr[\boldsymbol{R}] = \mu \frac{n}{N} \tag{17}$$

The mean square error ξ is

$$\xi = \xi_{min}(1 + M) = \left(1 + \frac{\mu n}{N}\right)\left(\frac{1}{N}\sum_{j=n}^{N-1} kl_j^2 + E[n_k^2]\right) \tag{18}$$

The MSE thus depends on the noise power, the power in the ST-T complex not represented by the first n kl_n coefficients and the gain constant μ. Note that the dependence on the KLT order n is not strong, as an increase in n value increases the $(1 + (\mu n/N))$ factor and decreases the $\sum_{j=n}^{N-1} kl_j^2$ factor. Thus, the optimum solution minimises n and maximises $\sum_{j=0}^{n-1} kl_j^2$; this property is intrinsic to the KLT. Given that, at the steady state, the estimated signal y_k is orthogonal to the error e_k (WIDROW and STEARNS, 1985), the *ExcessMSE* is the excess of error power introduced in y_k, and the signal-to-noise ratio of this estimation SNR_y, will be

$$SNR_y = \frac{\frac{1}{N}\sum_{j=0}^{n-1} kl_j^2}{\left(\frac{\mu n}{N}\right)\left(\frac{1}{N}\sum_{j=n}^{N-1} kl_j^2 + E[n_k^2]\right)} \tag{19}$$

If we consider that the ST-T energy is strongly concentrated in the first n coefficients, we can neglect the term $\sum_{j=n}^{N-1} kl_j^2$, obtaining

$$SNR_y = \frac{\frac{1}{N}\sum_{j=0}^{N-1} kl_j^2}{\left(\frac{\mu n}{N}\right)E[n_k^2]} \simeq SNR_d \frac{N}{\mu n} \tag{20}$$

where SNR_d is the SNR of the original signal. Comparison of this SNR_y with that obtained from the direct estimation of $kl_n(i)$ will give the SNR improvement ΔSNR achieved by the adaptive system. Direct $kl_n(i)$ estimation yields a signal-to-noise ratio, SNR_y^{direct}, that can be estimated if we assume the noise is white and that its PSD is uniformly distributed in the KLT domain:

$$SNR_y^{direct} = \frac{\frac{1}{N}\sum_{j=0}^{n-1} kl_j^2}{E[n_k^2]\frac{n}{N}} \simeq SNR_d \frac{N}{n} \tag{21}$$

Thus the SNR improvement obtained using the adaptive filter is

$$\Delta SNR = \frac{SNR_y}{SNR_y^{direct}} = \frac{1}{\mu} \tag{22}$$

Thus we find that, for appropriately chosen values of μ, the adaptive estimate of $kl_n(i)$ is cleaner than a $kl_n(i)$ time series obtained directly from the inner product. The choice of μ involves the typical trade-off between stability and rate of convergence, which limits the amount of improvement that can be obtained in practice, given the need to track changes occurring within a few beats in typical cases. When the interest of the estimation is in the ischaemic changes that occur gradually from beat to beat the convergence restriction will be that it occurs in a reduced number of beats. The next Section will consider the real-case election.

3.2 *Application to real signals with ischaemic episodes*

In this Section, we present the results of estimating and monitoring the $kl_n(i)$ values on several real ECG records. The parameters that we have selected for the adaptive estimate are $\mu = 0.1$, with $n = 4$ $kl_n(i)$ functions and $N = 150$. These values do not approach the convergence limit $\mu_{lim} = 12.5$, and give a time constant $\tau_{mse} = N/4\mu = 375 = 2.5$ beats. This convergence time is reasonable for monitoring ischaemic ST changes that typically occur over much longer intervals. The ΔSNR obtained in this case is $1/\mu = 10$ dB, representing a large improvement in the $kl_n(i)$ estimation.

The real signals are taken from the European ST-T database (TADDEI *et al.*, 1992). This database contains records manually annotated by clinical experts who identified episodes of significant ST-T changes consistent with ischaemia. The database was designed to provide a resource for the development and evaluation of automated ischaemia detectors. All of the patient records in the database have been analysed with our KLT technique, and its performance is illustrated by several selected cases chosen to illustrate the properties of the KLT technique.

To assist in the interpretation of the kl coefficients, we show in Fig. 5 the kl_0 time series from the ECG of a patient during percutaneous transluminal coronary angioplasty (PTCA). The ST-T complex shows marked morphological variations from inflation to post-inflation. Note how, during the first period (balloon inflation), the ST segment is positive, as is kl_0. During the post-inflation period, the ST-T complex inverts its amplitude and oscillates in magnitude. This is reflected in the kl_0 series as an oscillating negative value of the kl_0 coefficients.

Fig. 6 illustrates $kl_n(i)$ time series, each 2 h in length, for three ECG records from the European ST-T database. Fig. 6*a* compares the $kl_0(i)$ series of record e0103 for each of the two recorded ECG leads, estimated as the inner product between the ST-T complex and the first (uncorrected) KLT basis function. Fig. 6*b* shows the same series, obtained using the adaptive estimate with the parameters as given above, and showing a ΔSNR of about 10 dB compared with those of Fig. 6*a*. Note the simultaneous appearance of ischaemic ST-T changes in both leads, which is repeated quasi-periodically. Note also the similarity of the temporal pattern of sequential ischaemic episodes.

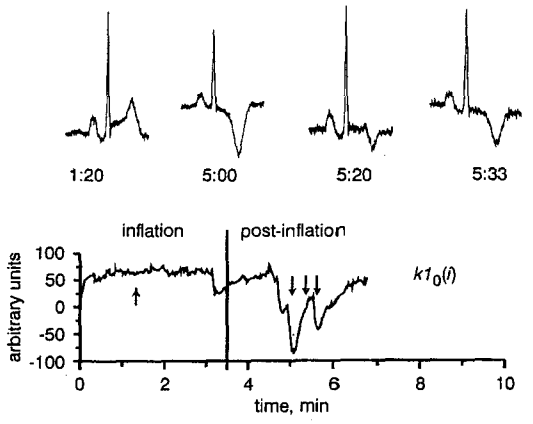

Fig. 5 *Example of time series of first kl coefficient kl_0, from patient with large ST-T variations during PTCA. Four sample beats are shown at top of Figure, corresponding to times indicated by arrows on $kl_0(i)$ series. Note how, during balloon inflation period, ST-T complex is positive, corresponding to positive kl_0 values. After deflation of balloon, ST-T complex inverts polarity and oscillates in magnitude. This is reflected in kl_0 time series as negative oscillating value*

The Figure clearly shows eight ischaemic episodes, corresponding to the eight peaks in the $kl_n(i)$ time series. Only five of these are marked in the database reference annotations, as three of these episodes (first, second, and seventh) are below the standard thresholds for defining ischaemic ST-T episodes. The technique we present allows these sub-threshold episodes to be identified unambiguously, and allows the long-term pattern of quasi-periodic ischaemic changes to be observed more clearly than would be possible otherwise. As the time series are initialised to zero, the time required for the adaptive algorithm to reach steady state (at the left edge of Figs. 6*b*, *d* and *f*) can be seen to be negligible in comparison with the evolution of the ischaemic variations.

Fig. 6*c* shows the $kl_0(i)$ (left) and $kl_1(i)$ (right) series of the ECG signal (only lead MLIII) of record e0105, and Fig. 6*d* shows their adaptively estimated counterparts. In this case, each of the seven peaks corresponds to an ischaemic ST-T episode marked in the database reference annotations. By study of two or more KLT coefficients in a single lead, we can easily monitor changes in ST-T morphology. Note how the ST segment elevation that corresponds to potential ischaemia in the e0105 record results in increased $kl_0(i)$ values and decreased (negative) $kl_1(i)$ values, as pointed out in Section 2.1. Note again that the temporal pattern of each ischaemic episode is quite constant.

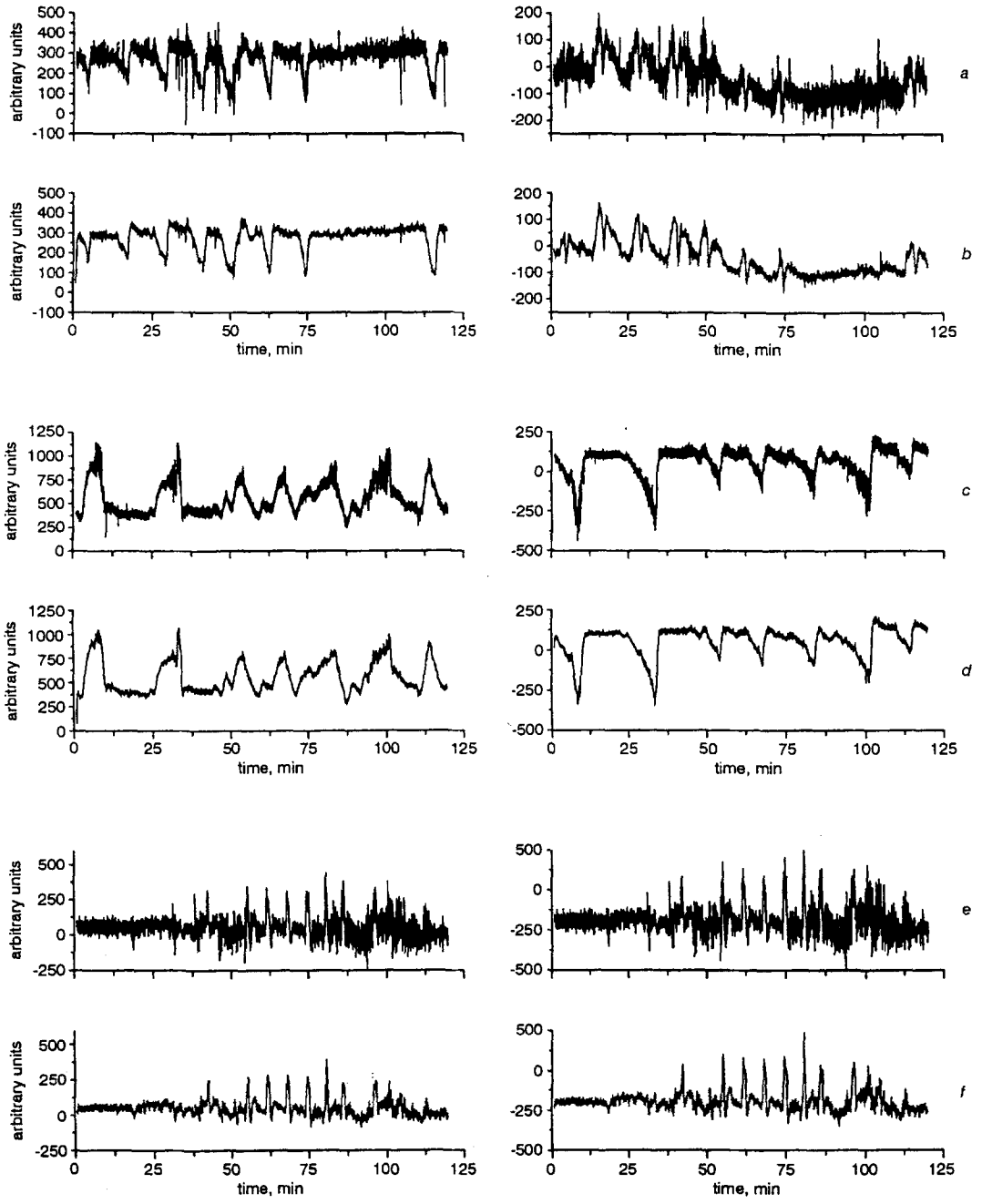

Fig. 6 *$kl_n(i)$ plots for three records of European ST-T database. (a), (b) $kl_0(i)$ time series of record e0103 (a) estimated directly from inner product, and (b) with adaptive estimate; those on left correspond to first lead (V4); those on right correspond to second lead (MLIII). (c), (d) $kl_0(i)$ time series for record e0105 on left, and $kl_1(i)$ time series for same lead (MLIII) on right. (e), (f) Uncorrected $kl_0(i)$ time series for record e0113 on left, and corresponding HR-corrected $kl_0(i)$ time series on right for same lead (MLIII). Temporal axes reflect time instant at which beat, corresponding to kl value, appears*

Finally, in Fig. 6*e*, the uncorrected and HR-corrected $kl_0(i)$ time series for the first ECG signal of record e0113 are shown, and Fig. 6*f* shows their adaptively estimated counterparts. As in the previous examples, the adaptive estimation of ST morphology tracks ischaemic changes noted in the reference annotation files of the database. Note the slightly higher amplitude of the peaks in the HR-corrected series, showing that the first corrected $kl_n(i)$ basis function is better able to represent the ST-T complexes in this record than is the first uncorrected $kl_n(i)$ basis function. In Fig. 6*f* we note that, of the eight well-marked peaks, seven correspond to ischaemic episodes annotated in the database, but one other (the second) was not so annotated in the database, although its presence is quite clear from inspection of the $kl_n(i)$ series.

In the examples presented in Fig. 6, it can be seen that both traces (adaptive and inner product estimated) reflect the ST-T changes. However, when the changes are not as clearly defined (first salvo in Figs. 6*a* and *b* and last in Figs. 6*e* and *f*), the adaptive estimation is more suited. In addition, where automatic ischaemia detection is concerned, the influence of noise decreases the sensitivity and specificity of the inner product with respect to those of the adaptive estimate.

Analysing the entire European ST-T database (90 records), we found that roughly 20% of the records demonstrated the quasi-periodic salvos of ST-T changes shown in Fig. 6. In most records containing multiple ST-T variation episodes, we noted similarity in the temporal structure of their $kl_n(i)$ time series, suggesting a similar pathophysiological mechanism. It is clear that the KLT technique detects and locates transient ST-T variations. Subsequent detailed analysis of the record and/or collateral clinical information should be used to determine whether the ST-T variations are actually associated with ischaemic episodes.

This technique has been used to design an automatic ischaemia detector (GRACIA, 1998), making use of the first four *kl* series. The automatic detector can be configured to detect either the ST segment, T-wave or ST-T complex episodes (for the detector validation, we used the manual annotations in ST segment and T-wave from the European ST-T database and the OR combination of ST and T episodes for the ST-T complex (TADDEI *et al.*, 1992)). The preliminary results obtained in terms of sensitivity S and positive predictivity $+P$ are $S=81\%$ and $+P=80\%$, when detecting ST episodes. This shows a very good performance of the technique which can help clinicians in ischaemic episode detection in Holter ECGs and may be useful for alarm design in coronary care units.

3.3 $kl_n(i)$ series compared with $qt(i)$ series

Repolarisation is reflected in both the shape of the ST-T waveform and also in the duration of the QT interval. We compared the $kl_n(i)$ time series, with the $qt(i)$ time series using the techniques for QT estimation described elsewhere (LAGUNA *et al.*, 1994). An example from record e0103 is shown in Fig. 7. In this case, the ischaemic episodes are clearly manifested in the $kl_n(i)$ time series. The $qt(i)$ time series taken from lead III (but not that taken from lead V4) shows transient increases in the QT interval during the first four ischaemic episodes (but not the last three). The QT variations persisted after correction for heart rate using Bazett's formula.

Fig. 8 shows that the transient QT prolongation accompanies ischaemic ST-T episodes (Fig. 8*c*), and becomes even more prominent after correction for heart rate (Fig. 8*d*).

Analysing the entire European ST-T database (90 records), we found that roughly 50% of ischaemic records showed QT variations in at least one lead associated with the ischaemic episodes.

3.4 $kl_n(i)$ series compared with $st(i)$ series

To show the differences between conventional ST level monitoring and the *kl* series monitoring we created ST level trend plots for several records and compared them with corresponding *kl* time series. The weighted averaging method was used to measure the ST segment deviations. This method is especially useful when the beat-to-beat noise level changes.

ST segments were selected from averaged ECG complexes. To ensure convergence properties similar to those of the KLT estimation method previously described, only three beats were included in each sub-ensemble average. Also only normal beats surrounded by normal beats were included, to avoid artefacts. Each beat was added into the average with a weighting factor inversely proportional to its noise content. The weighted average (ZHONG and LU, 1991) is given by

$$\bar{x}(t) = \sum_{i=1}^{N_{beat}} w_i x_i(t) \tag{23}$$

where N_{beat} is the number of beats to be averaged, x_i is the ith beat, and w_i is the weight applied to that beat. For simple signal averaging $w_i = 1/N_{beat}$, i.e. each beat has an equal weight. The weighting factor is

$$w_i = \left(\frac{1}{\sigma_i^2}\right)\left(\frac{1}{\sum_{j=1}^{N_{beat}} \frac{1}{\sigma_j^2}}\right) \tag{24}$$

where σ_i^2 is the noise power of the ith beat. Once each three-beat average had been constructed, the ST level was measured by taking the mean value in a 10 ms interval, centred 60 ms from the end of the QRS.

In Fig. 9*a*, we show the kl_0 series of record e0129 (two leads) and, in Fig. 9*b*, we show the corresponding ST level series for each lead. Note the significant enhancement of the ST episodes by the KLT method, especially in lead V3. Fig. 10 shows similar plots for record e0103, and again the superiority of the *kl* trend plots is clear. From these examples and others throughout the ESC ST-T database, we confirmed our expectation that the KLT technique is much more robust and sensitive than the single ST level measure.

3.5 ST-T alternans detection from $kl_n(i)$ series

The KLT can also be used to detect alternans in the ST-T complex. Alternans can be an index of the risk of SCD (CLANCY *et al.*, 1991; ROSENBAUM *et al.*, 1994). We calculate a spectrum from the series of KLT coefficients, with the independent variable being the beat number. The spectrum obtained in this way is a beat spectrum (DEBOER *et al.*, 1984) rather than a frequency spectrum; the units corresponding to frequency are cycles per beat (beat^{-1}). This spectrum is best suited for the study of alternans, as we are interested in beat periodicities rather than the time periodicities that require study of frequency spectra.

Fig. 11 illustrates the detection of subtle alternans in record e0105 of the European ST-T database using the $kl_n(i)$ series and its beat spectrum. This record presents alternans in association with the ST-T variation (potentially ischaemic) episodes shown in Fig. 6.

Fig. 11*a* shows beat-to-beat alternation of ST-T morphology during the first ST-T variation episode. Fig. 11*b* shows the $kl_0(i)$ series calculated directly (at left) and its beat spectrum (at

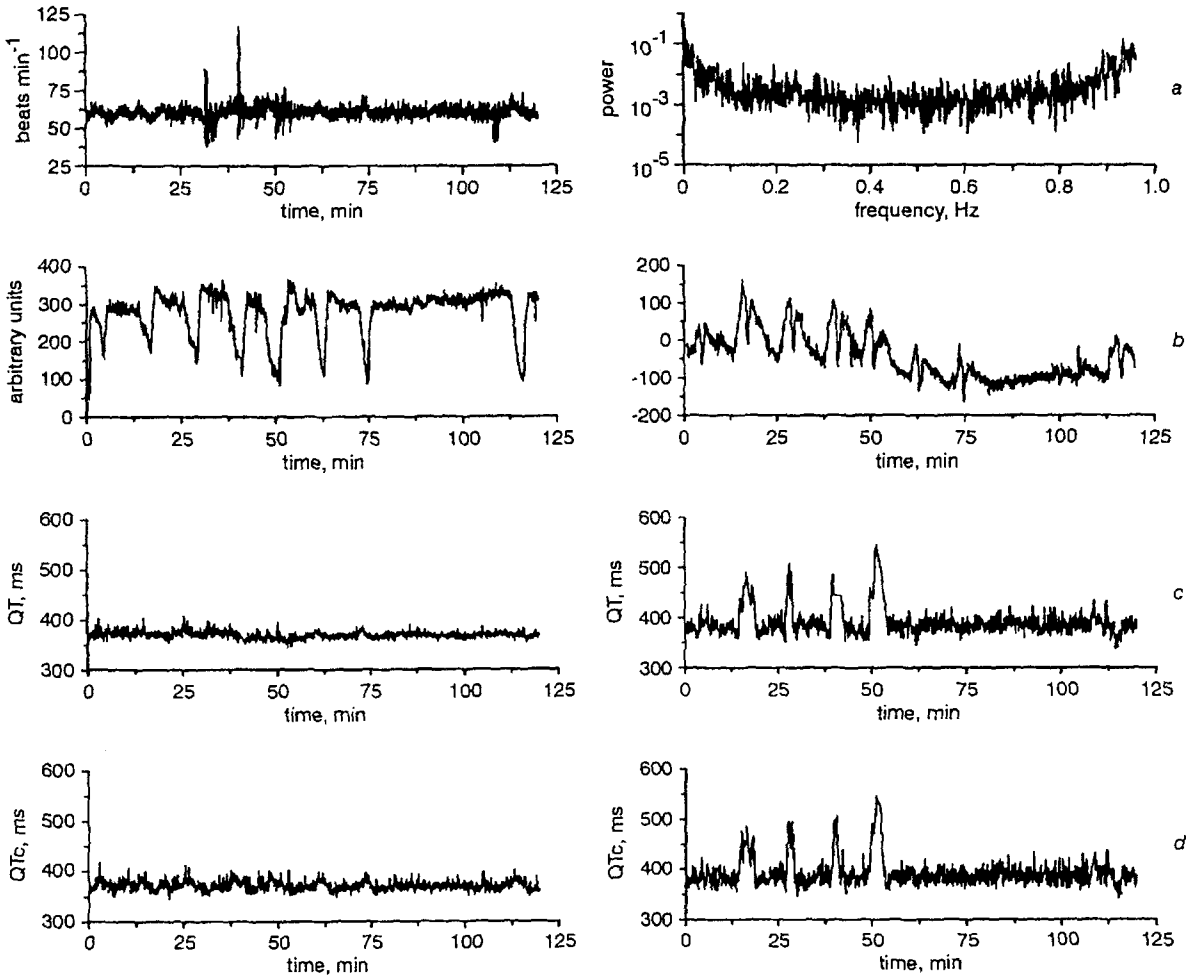

Fig. 7 *kl and qt plots for record e0103 of European ST-T database. (a) Heart rate (left) and its power spectrum density (right) estimated with Lomb spectrum[32] (only frequencies up to inverse mean heart period are meaningful); (b) kl_0 time series estimated with adaptive filter for lead V4 (left) and lead MLIII (right); (c) qt series for both leads estimated as mean after rejecting maximum and minimum values in five beat sets. (d) Bazett's corrected qt series*

right). The clear peak at 0.5 beat^{-1} represents the periodic beat-to-beat ST-T shape variations, visible in the time series as a high-frequency, high-amplitude modulation near the middle of the 15 min series. In addition, the beat spectrum reveals the appearance of a 0.25 beat^{-1} peak associated with a period 4 variation in ST-T morphology, also observable in Fig. 11*a*.

There is another peak at 0.0 beat^{-1} and its harmonic at 1.0 beat^{-1} that represent a DC component over the entire $kl_n(i)$ series. This comes from the overall $kl_n(i)$ variation due to the underlying ischaemic evolution.

Figs. 11*c* and *d* show another episode of alternans, occurring during the sixth ST-T variation episode of the record (see Figs. 6*c* and *d*). In this episode, both period 2 and period 4 alternans are even more marked than in the first example. Although the alternans can be detected even when adaptive $kl_n(i)$ estimates are used (Fig. 11*e*), the resulting attenuation of short-term variation makes it clear that the directly estimated $kl_n(i)$ series is better suited for this purpose.

Fig. 11*f* (left) shows the HR spectrum, obtained using a technique for power spectral density estimation of irregularly sampled signals (LAGUNA *et al.*, 1998); this spectrum confirms that the alternans is not an artefact of an underlying HR modulation. Fig. 11*f* (right) shows the $kl_n(i)$ frequency spectrum, estimated using the same technique; the alternans is less apparent in this frequency spectrum than in the beat spectra, as a result of the change in HR that makes the alternans not strictly time periodic. The beat spectrum (Fig. 11*d*, right) of the $kl_n(i)$ is thus much more appropriate for alternans detection than the time spectrum (Fig. 11*f*, right).

Finally, Figs. 11*g* and *h* show this analysis during a non-ischaemic period of the same record. In this case, the beat-to beat alternans has almost disappeared, but the period 4 alternans remains apparent.

By study of the entire record, we can observe that the period 2 alternans appears in association with the ST-T variation episodes, usually in the later portions of each episode, but disappears rapidly during recovery. The period 4 alternans is also associated with the ST-T varying episodes, but persists after recovery. It seems that the period 4 alternans is more prominent in the non-ischaemic periods (Fig. 11*h*) than during ischaemic periods (Fig. 11*d*). This happens because the total power is normalised to unity, and then, when the period 2 disappears, most of the relevant energy is at period 4. The interpretation should be made in relative terms rather than absolute.

Based on this 'beatquency' spectrum and KLT series, we developed an alternans detector (LAGUNA *et al.*, 1996*b*) that detects alternans representing around 60 μV amplitude variations of the ST-T complex. A detailed analysis of the European ST-T database has shown that about 5% of ischaemic episodes present alternans associated with them, and, also, more than 50% of the alternans present in the recordings are associated

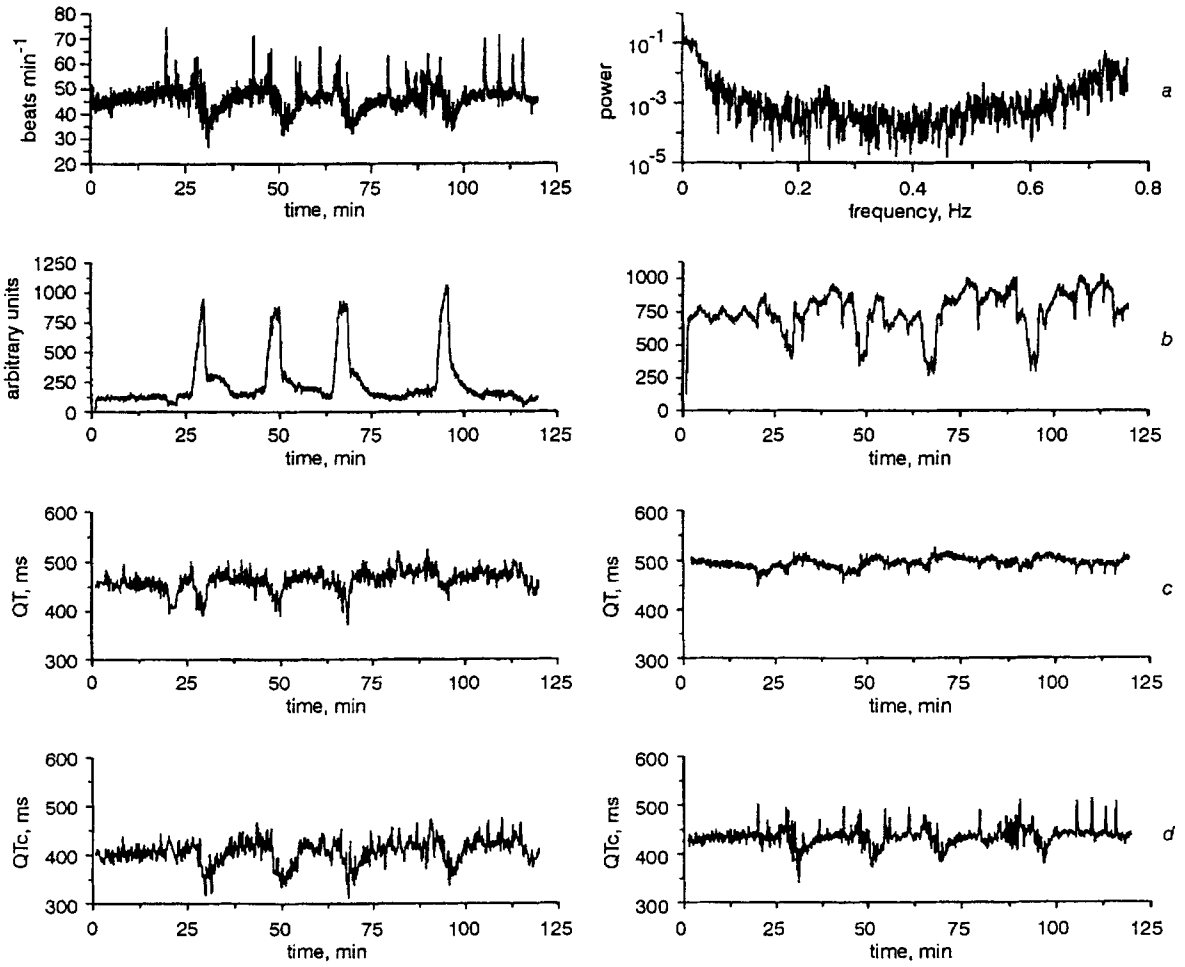

Fig. 8 *$kl_n(i)$ and $qt(i)$ plots for record e0129 of European ST-T database. (a) Heart rate (left) and its power spectrum density (right) estimated with Lomb spectrum (LAGUNA et al., 1998) (only frequencies up to inverse mean heart period are meaningful); (b) $kl_0(i)$ time series estimated with adaptive filter for lead MLIII (left) and lead V3 (right); (c) $qt(i)$ series for both leads estimated as mean after rejecting maximum and minimum values in five beat sets. (d) Bazett's corrected $qt(i)$ series*

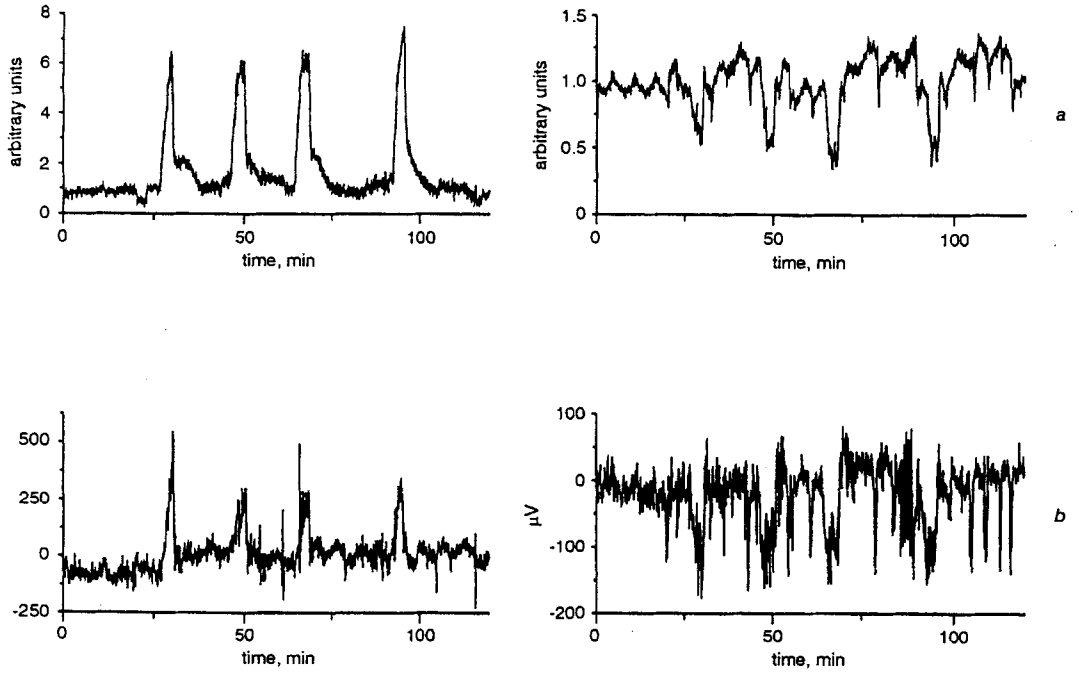

Fig. 9 *$kl_n(i)$ and $st(i)$ plots for record e0129 of European ST-T database. (a) $kl_0(i)$ time series estimated with adaptive filter for lead MLIII (left) and lead V3 (right); (b) $st(i)$ series for both leads estimated as described in text*

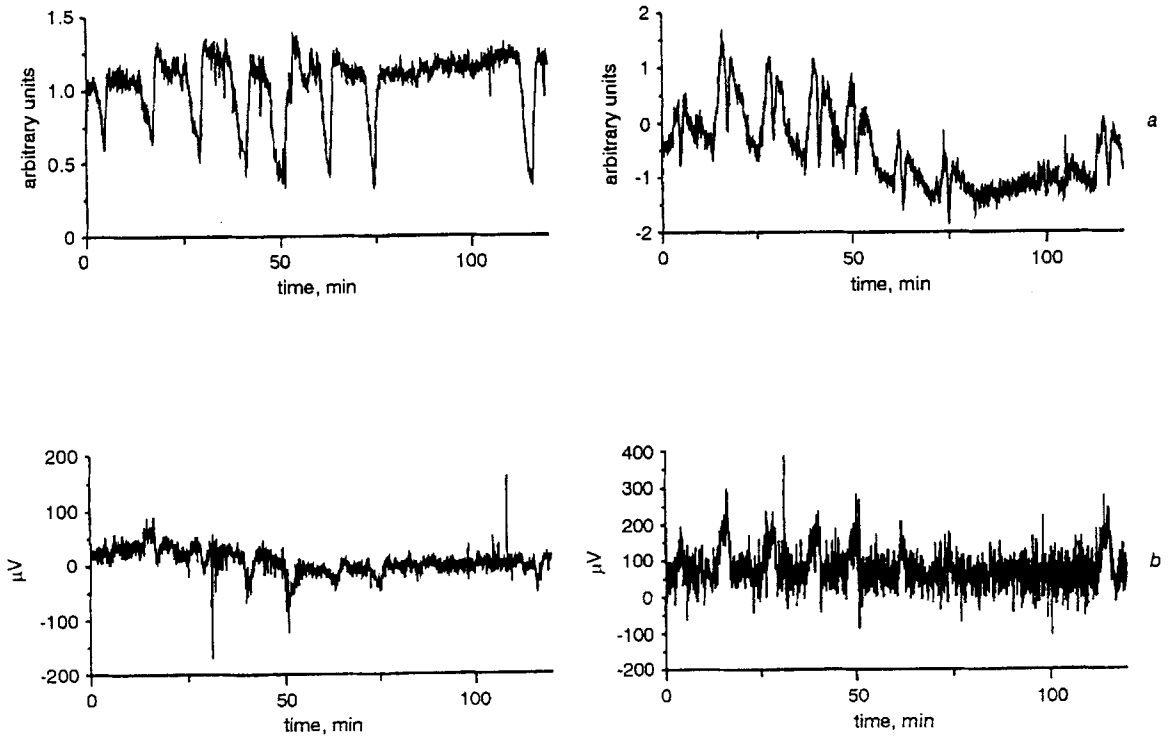

Fig. 10 *$kl_n(i)$ and $st(i)$ plots for record e0103 of European ST-T database. (a) $kl_0(i)$ time series estimated with adaptive filter for lead V4 (left) and lead MLIII (right); (b) $st(i)$ series for both leads estimated as described in text*

with the ischaemic episodes (LAGUNA *et al.*, 1996*b*). This corroborates previous clinical works that relate the alternans phenomena strongly with the ischaemia. This detector can be used as a new index when analysing Holter ECG recordings to prevent ventricular arrythmias.

4 Discussion and conclusions

In this work, we have presented a KLT technique for studying the repolarisation period of the heart throughout the ST-T complex of the ECG signal. We have developed a KLT training set of ST-T complexes, containing a broad range of morphologies, to obtain the KLT basis vectors. We have shown that this representation permits about 90% of the signal energy to be represented by the first four $kl_n(i)$ coefficients.

We have shown that heart rate correction of the ST-T complex using Bazett's formula improves the performance of the KLT, whereas neither linear high-pass nor linear bandpass filtering has any beneficial effect. The KLT has been used to detect ST-T shape variations, with results demonstrating its sensitivity for detecting ST variations (potentially related to ischaemic events).

We have described an adaptive filter, based on the adaptive linear combiner with the LMS algorithm, for improving the signal-to-noise ratio of a time series of KLT coefficients. The adaptive estimation system delivers an improvement of about 10 dB for a practical choice of parameters for monitoring ischaemic ST-T changes. The direct estimates of the KLT coefficient time series and beat spectra derived from them have been shown to be well suited for study of ST-T alternans.

In demonstrating the application of these techniques to analysis of the entire European ST-T database, we have shown that about 20% of the records reveal a quasi-periodic pattern of ischaemic ST-T episodes, and another 20% exhibit repetitive, but not clearly periodic, patterns of ST-T change episodes. These observations are drawn from information coming from the entire ST-T complex; it would be difficult, if not impossible, to reach similar conclusions with confidence using classical differential measurements of ventricular repolarisation, such as measurements of ST level or QT interval.

The salvo patterns of ischaemia suggest an oscillatory or periodic instability of the coronary blood supply, perhaps due to cyclic vasospasm. More study of the phenomenon is warranted, as the temporal patterns of ischaemia may guide therapeutic interventions. Preliminary results on automatic ischaemia detection using four *kl* coefficients give a sensitivity of 81% and a positive predictivity of 80% for the European ST-T database.

Finally, we have observed alternans of periods 2 and 4 in association with ischaemic episodes, with different responses to recovery. Period 4 alternans and the association of alternans with ST-T changes (ischaemia) have not been previously reported; the techniques we describe make the study of these phenomena possible. However a complementary analysis of the respiration will be required to establish whether the period 4 alternans are a result of the respiration rate coupled with HR or are intrinsic period 4 alternans. A complete analysis of the European ST-T database reveals that 5% of the ischaemic episodes present period 2 alternans associated with them.

The KLT technique can be used for long-term tracking of ST-T variations and may open the door for development of improved automatic detectors of transient ST-T changes.

Acknowledgments—This work was supported in part by project TIC97-0945-C02-02 from CICYT, a personal grant to P.L. from the 'Instituto Aragones de Fomento (IAF)' (Spain) and by grants from the G. Harold and Leila Y. Mathers Charitable Foundation and the National Aeronautics & Space Administration (USA).

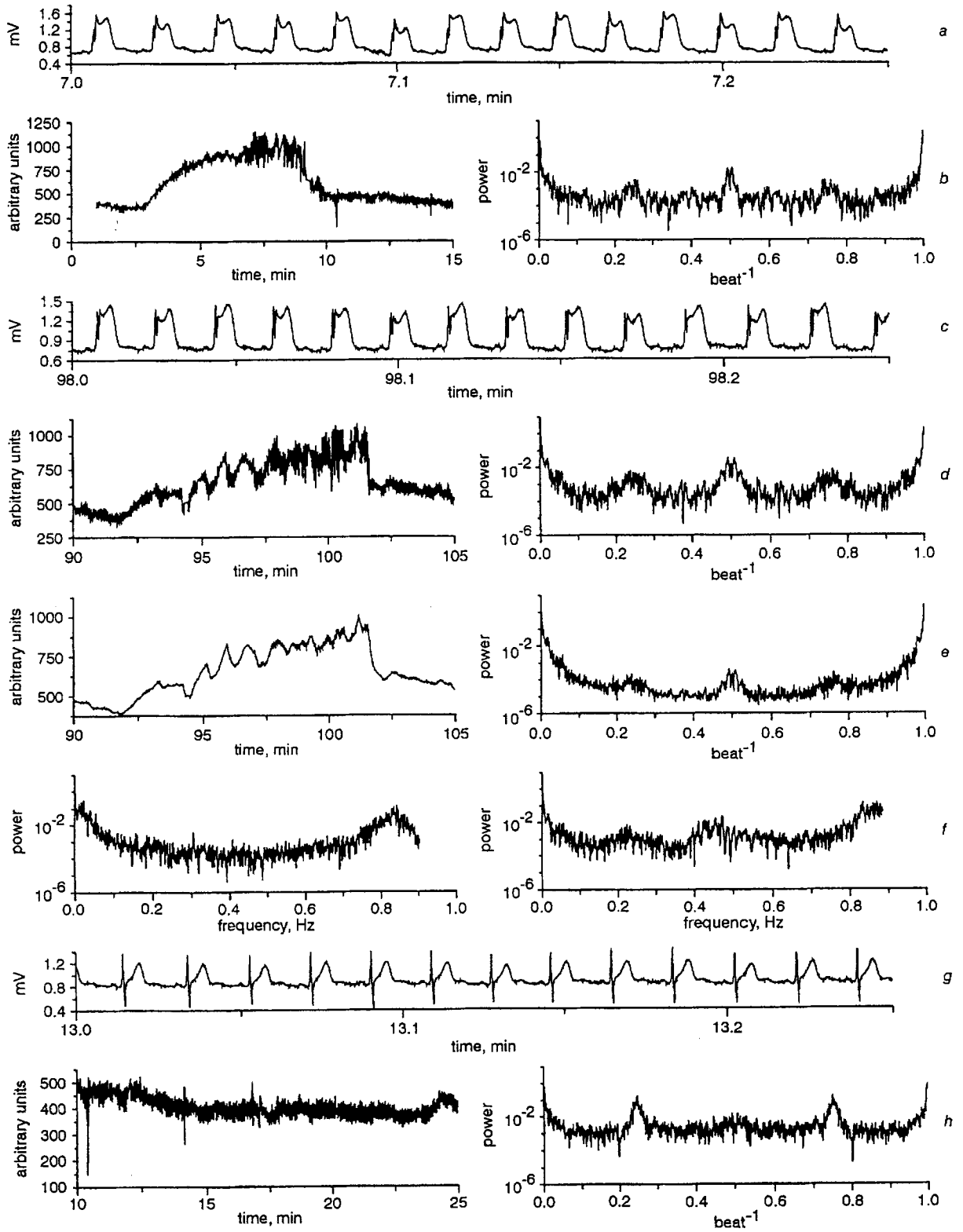

Fig. 11 *Alternans in record e0105 of European ST-T database. (a) ECG during first ischaemic ST-T episode; (b) $kl_0(i)$ time series during 15 min interval, including ischaemic episode, and corresponding beat spectrum. Beat spectrum exhibits clear peak corresponding to period 2 alternans (at 0.5 beat^{-1}), and also shows period 4 alternans (at 0.25 beat^{-1}). (c) Excerpt of ECG during another ischaemic episode; (d) corresponding $kl_0(i)$ time series and beat spectrum; (e) same data, derived using adaptive estimation. Adaptive estimate attenuates beat-to-beat variations; it is better suited for study of longer-term variations. (f) HR power spectrum and $kl_0(i)$ frequency spectrum for same interval (see text). (g), (h) Excerpt of ECG, a $kl_0(i)$ time series and corresponding beat spectrum during non-ischaemic period in same record, where period 2 alternans has disappeared, but a period 4 alternans remains*

References

AKSELROD, S., NORYMBERG, M., PELED, I., KARABELNIK, E., and GREEN, M. S. (1987): 'Computerized analysis of ST segment changes in ambulatory electrocardiograms', *Med. Biol. Eng. Comput.*, **25**, pp. 513–519

BAZZETT, H. C. (1920): 'An analysis of the time relation of electrocardiograms', *Heart*, **7**, pp. 353–370

BERBARI, E., and LAZZARA, R. (1988): 'An introduction to high-resolution ECG recordings of cardiac late potentials', *Arch. Intern. Med.*, **148**, pp. 1859–1863

BREITHARDT, G., CAIN, M. E., EL-SHERIF, N., FLOWERS, N., HOMBACH, V., JANSE, M. SIMSON, M., and STEINBECK, G. (1991): 'Standards for analysis of ventricular late potentials using high resolution or signal-averaged electrocardiography', *J. Am. Coll. Cardiol.*, **17**, pp. 999–1006

CLANCY, E. A., SMITH, J. M., and COHEN, R. J. (1991): 'A simple electrical–mechanical model of the heart applied to the study of electrical–mechanical alternans', *IEEE Trans.*, **BME-38**, (6), pp. 551–560

DEBOER, R. W., KAREMAKER, J. M., and STRACKEE, J. (1984): 'Comparative spectra of series of point element particularly for heart rate variability data', *IEEE Trans.*, **BME-31**, pp. 384–387

FEUER, A., and WEINSTEIN, E. (1985): 'Convergence analysis of LMS filters with uncorrelated Gaussian data', *IEEE Trans. Acoust. Speech Signal Process.*, **33**, pp. 222–230

GALLINO, A., CHIERCHIA, S., SMITH, G., CROOM, M., MORGAN, M., MARCHESI, C., and MASERI, A. (1984): 'Computer system for analysis of ST segment changes on 24 hour Holter monitor tapes: Comparison with other available systems', *J. Am. Coll. Cardiol.*, **4**, (2), pp. 245–252

GRACIA, J. (1998): *'Sistema de monitorización y detección de isquemia basado en la transformada de Karhunen–Loève aplicada sobre el ECG* (in Spanish). Ph.D. thesis, Universidad de Zaragoza, Zaragoza

HADDAD, R. A., and PARSONS, T. W. (1991): *'Digital signal processing. Theory, applications and hardward'* (Computer Science Press, New York)

JAGER, F. J., MARK, R. G., MOODY, G. B., and DIVJAK, S. (1992): 'Analysis of transient ST segment changes during ambulatory monitoring using the Karhunen–Loève transform', *in 'Computers in cardiology'* (IEEE Computer Society Press) pp. 691–694

KLIEGER, R. E., MILLER, J. P., BIGGER, J. T., and MOSS, A. M. (1984): 'Heart rate variability: a variable predicting mortality following acute myocardial infarction', *J. Coll. Cardiol.*, **3**, p. 2

LAGUNA, P., JANÉ, R., and CAMINAL, P. (1994):'Automatic detection of wave boundaries in multilead ECG signals: Validation with the CSE database', *Comput. Biomed. Res.*, **27**, (1), pp. 45–60

LAGUNA, P., JANÉ, R., MESTE, O., POON, P. W., CAMINAL, P., RIX, H., and THAKOR, N. V. (1992): 'Adaptive filter for event-related bioelectric signals using an impulse correlated reference input: comparison with signal averaging techniques', *IEEE Trans.*, **BME-39**, (10), pp. 1032–1044

LAGUNA, P., JANÉ, R., OLMOS, S., THAKOR, N. V., RIX, H., and CAMINAL, P. (1996*a*): 'Adaptive estimation of QRS complex by the Hermite model for classification and ectopic beat detection', *Med. Biol. Eng. Comput.*, **34**, pp. 58–68

LAGUNA, P., RUIZ, M., MOODY, G. B., and MARK, R. G. (1996*b*): 'Repolarization alternans detection using the KL transform and the beatquency spectrum', *in 'Computers in cardiology'* (IEEE Computer Society Press) pp. 673–676

LAGUNA, P., MARK, R., GOLDBERGER, A., and MOODY, G. (1997): 'A database for evaluation of algorithms for measurement of QT and other waveform intervals in the ECG', *in 'Computers in cardiology'* (IEEE Computer Society Press)

LAGUNA, P., MOODY, G. B., and MARK, R. (1998): 'Power spectral density of unevenly sampled data by least-square analysis: Performance and application to heart rate signals', *IEEE Trans. Signal Process.*, **45**, (6), pp. 698–715

LYNN, P. A. (1977): 'Online digital filters for biological signals: Some fast designs for a small computer', *Med. Biol. Eng. Comput.*, **15**, pp. 534–540

MERRI, M., ALBERTI, M., and MOSS, A. J. (1993): 'Dynamic analysis of ventricular repolarization duration from 24-hour Holter recordings', *IEEE Trans.*, **BME-40**, (20), pp. 1219–1225

MEYER, C. R., and KEISER, H. N. (1977): 'Electrocardiogram baseline noise estimation and removal using cubic splines and state-space computation techniques', *Comput. Biomed. Res.*, **10**, pp. 459–470

MOODY, G. B., and MARK, R. G. (1982): 'Development and evaluation of a 2-lead ECG analysis program', *in 'Computers in cardiology'* (IEEE Computer Society Press) pp. 39–44

MOODY, G. B., and MARK, R. G. (1990*a*): 'The MIT-BIH arrhythmia database on CD-ROM and software for use with it', *in 'Computers in cardiology'* (IEEE Computer Society Press) pp. 185–188

MOODY, G. B., and MARK, R. G. (1990*b*): 'QRS morphology representation and noise estimation using the Karhunen–Loève transform', *in 'Computers in cardiology'* (IEEE Computer Society Press) pp. 269–272

MYERS, G., MARTIN, G., MAGID, N., BARNETT, P., SCHAAD, J., WEISS, J., LESCH M., and SINGER, D. H. (1986): 'Power spectral analysis of heart rate variability in sudden cardiac death: comparison to other methods', *IEEE Trans.*, **BME-33**, (12), pp. 1149–1156

PUDDU, P. E., and BOURASSA, M. G. (1986): 'Prediction of sudden death from QTc interval prolongation in patients with chronic ischemic disease', *J. Electrocardiol.*, **19**, (3), pp. 203–212

ROSENBAUM, D. S., JACKSON, L. E., SMITH, J. M., GARAN, H., RUSKIN, J. N., and COHEN, R. J. (1994): 'Electrical alternans and vulnerability to ventricular arrhythmias', *New Engl. J. med.*, **330**, (4), pp. 235–241

SPERANZA, G., NOLLO, G., RAVELLI, F., and ANTOLINI, R. (1993): 'Beat-to beat measurement and analysis of the R-T interval in 24 h ECG Holter recordings,' *Med. Biol. Eng. Comput.*, **31**, (5), pp. 487–494

TADDEI, A., DISTANTE, G., EMDIN, M., PISANI, P., MOODY, G. B., ZEELENBERG, C., and MARCHESI, C. (1992): 'The European ST-T database: standards for evaluating systems for the analysis of ST-T changes in ambulatory electrocardiography', *Eur. Heart J.*, **13**, pp. 1164–1172

THAKOR, N. V., GUO, X., VAZ, C. A., LAGUNA, P., JANÉ, R., CAMINAL, P., RIX, H., and HANLEY, D. (1993): 'Orthonormal (Fourier and Walsh) models of time-varying evoked potentials in neurological injury', *IEEE Trans.*, **BME-40**, (3), pp. 213–221

THAKOR, N. V., WEBSTER, J. G., and TOMPKINS, W. J. (1984): 'Estimation of QRS complex power spectrum for design of a QRS filter', *IEEE Trans.*, **BME-31**, (11), pp. 702–706

WIDROW, B., and STEARNS, S. D. (1985): *'Adaptive signal processing'* (Prentice-Hall, Englewood Cliffs, New Jersey)

ZHONG, J., and LU, W. (1991): 'On two weighted signal averaging methods and their application to the surface detection of cardiac micropotentials', *Comput. Biomed. Res.*, **24**, pp. 332–343

Author's biography

PABLO LAGUNA was born in Jaca (Huesca), Spain in 1962. He received his Physics degree (MS) and PhD from the University of Zaragoza, Spain, in 1985 and 1990, respectively. His PhD thesis was developed at the Biomedical Engineering Division of the Institute of Cybernetics (I.C.), Politecnic University of Catalonia (U.P.C.)–C.S.I.C., Barcelona, Spain. He is currently Associated Professor of Signal Processing and Communications in the Department of Electronics Engineering and Communications at the Centro Politécnico Superor, U.Z. From 1987 to 1992 he worked as Assistant Professor in the Department of Control Engineering at the U.P.C., and as a Researcher at the Biomedical Engineering Division of the I.C. His research interests include signal processing, in particular, applied to biomedical applications.